

# Detection of far-infrared rotational lines of water vapour toward W Hydrae<sup>\*</sup>

David A. Neufeld<sup>1</sup>, Wesley Chen<sup>1</sup>, Gary J. Melnick<sup>2</sup>, Thijs de Graauw<sup>3</sup>, Helmut Feuchtgruber<sup>4,5</sup>, Leo Haser<sup>5</sup>, Dieter Lutz<sup>5</sup>, and Martin Harwit<sup>6</sup>

<sup>1</sup> Department of Physics and Astronomy, The Johns Hopkins University, 3400 N. Charles St., Baltimore, MD 21218, USA

<sup>2</sup> Harvard-Smithsonian Center for Astrophysics, 60 Garden St., Cambridge, MA 02138, USA

<sup>3</sup> SRON Laboratory for Space Research, Groningen University, The Netherlands

<sup>4</sup> ISO Science Operations Center, ESA, Villafranca, Spain

<sup>5</sup> Max Planck Institute for Extraterrestrial Physics, D-85740 Garching, Germany

<sup>6</sup> 511 H Street, SW, Washington, DC 20024-2725, USA

Received 1 July 1996 / Accepted 20 August 1996

**Abstract.** We report the first detection of thermal water vapour emission from a circumstellar outflow. We have observed four far-infrared rotational emission lines of water vapour and one water absorption feature toward the evolved star W Hydrae, using the Short Wavelength Spectrometer (SWS) of the Infrared Space Observatory (ISO). Three of the emission lines were observed in the instrument's Fabry-Perot mode at a resolving power  $\lambda/\Delta\lambda$  of approximately 30 000: the  $7_{25} - 6_{16}$  line at  $29.84 \mu\text{m}$ , the  $4_{41} - 3_{12}$  line at  $31.77 \mu\text{m}$ , and the  $4_{32} - 3_{03}$  line at  $40.69 \mu\text{m}$ . One additional emission line, the  $4_{41} - 4_{14}$  line at  $37.98 \mu\text{m}$ , and one absorption feature at  $38.08 \mu\text{m}$  that we attribute to a blend of the  $13_{13,0} - 13_{12,1}$  and the  $13_{13,1} - 13_{12,2}$  water lines were observed in grating mode at a resolving power of about 2 000. The observed emission line fluxes were  $3.2 \times 10^{-19}$ ,  $6.3 \times 10^{-19}$ ,  $2.3 \times 10^{-19}$  and  $2.8 \times 10^{-19} \text{ W cm}^{-2}$  respectively, and the equivalent width of the absorption feature was  $\sim 10 \text{ km s}^{-1}$ . To within the possible errors in the flux calibration, the observed emission line fluxes can be accounted for simultaneously by a model similar to that of Chen & Neufeld (1995), given a mass-loss rate in the range  $(0.5 - 3) \times 10^{-5} M_{\odot} \text{ yr}^{-1}$ . This range lies at least a factor  $\sim 2$  above an independent estimate of the mass-loss rate that may be derived from dynamical considerations, and at least a factor  $\sim 30$  above previous estimates based upon the interpretation of CO observations.

**Key words:** stars: circumstellar matter – stars: late-type – infrared: stars – molecular processes

## 1. Introduction

Circumstellar outflows have been widely observed around evolved stars of low photospheric temperature and low surface gravity. Such outflows are believed to occur when newly-formed dust grains within the outflowing material are accelerated by radiation pressure and in turn transfer outward momentum to the gas through collisions (Gilman 1972; Salpeter 1974; Kwok 1975). This momentum transfer is inevitably accompanied by frictional heating, which warms the outflowing gas and is balanced by radiative and adiabatic cooling. Theoretical models for oxygen-rich circumstellar outflows (Goldreich & Scoville 1976, hereafter GS76; Deguchi & Rieu 1990; Chen & Neufeld 1995, hereafter CN95) predict that water molecules will be abundant in the warm outflowing gas and that far-infrared rotational emissions from water will dominate the radiative cooling.

Although maser emissions from water molecules have been extensively observed in circumstellar outflows (e.g. Bowers & Hagen 1984, and references therein), the non-masing far-infrared emissions that are predicted to dominate the cooling of the gas have not been detected previously. In this paper, we report the first detection of such emissions from a circumstellar outflow. In §2, we describe observations of the oxygen-rich evolved star W Hya that we have carried out using the Short Wavelength Spectrometer (SWS; de Graauw et al. 1996) of the Infrared Space Observatory (ISO; Kessler et al. 1996). In §3, we present spectra of the four water emission lines and one absorption feature that were detected. In §4, we compare our observations with theoretical predictions for water line emissions from circumstellar envelopes.

## 2. Observations

All the observations reported here were carried out toward the oxygen-rich evolved star W Hya using the SWS of ISO during

---

\* Based on observations with ISO, an ESA project with instruments funded by ESA Member States (especially the PI countries: France, Germany, The Netherlands and the United Kingdom) and with the participation of ISAS and NASA. The SWS is a joint project of SRON and MPE.

**Table 1.** Emission line fluxes measured in W Hydrae

Transition	Wavelength ( $\mu\text{m}$ )	Integrated Line Flux ( $\text{W cm}^{-2}$ )	$v_{LSR}$ ( $\text{km s}^{-1}$ )
$7_{25} - 6_{16}$	29.8367	$3.2 \times 10^{-19}$	40
$4_{41} - 3_{12}$	31.7721	$6.3 \times 10^{-19}$	38
$4_{32} - 3_{03}$	40.6909	$2.3 \times 10^{-19}$	40
$4_{41} - 4_{14}$	37.9839	$2.8 \times 10^{-19}$	

the Performance Verification phase of the ISO mission. The spectra of three water emission lines were obtained in Fabry-Perot (FP) mode on 28 Jan 1996: the  $7_{25} - 6_{16}$  line at  $29.84 \mu\text{m}$ , the  $4_{41} - 3_{12}$  line at  $31.77 \mu\text{m}$ , and the  $4_{32} - 3_{03}$  line at  $40.69 \mu\text{m}$ . The integration times were 1160, 1407 and 3561 s respectively. An additional spectrum covering the wavelength range  $37.9 - 38.2 \mu\text{m}$  was obtained in grating (GR) mode on 12 Jan 1996 with an integration time of 98 s. The projected aperture sizes were  $17 \times 40$  and  $20 \times 33$  arcsec and the resolving powers  $\lambda/\Delta\lambda$  were approximately 30 000 and 2 000 respectively for observations in FP and GR mode.

### 3. Results

Unambiguous detections were obtained for each of the four water emission lines that we observed and for one absorption feature. Figure 1 shows the continuum-subtracted spectra for the three emission lines that were observed in FP mode. Because of uncertainties in the dark current in the detectors, the continuum flux cannot be determined accurately from the FP observations. Accordingly, we reduced the FP data by subtracting flat continua and fitting Lorentzian profiles to the continuum-subtracted line spectra. Figure 2 is the grating spectrum that we obtained for the purpose of flux calibration without the expectation that spectral features would be present; the fortuitous detection of two water lines in a spectrum covering just  $0.3 \mu\text{m}$  in a wavelength region that was selected so as *not* to contain strong spectral features is a dramatic demonstration that water lines are indeed ubiquitous in the far-infrared spectrum of this source.

Table 1 lists the rest wavelengths (Toth 1991), the integrated line fluxes and the LSR velocities at line center for the four emission lines. The absorption feature, which we attribute to a blend of the  $13_{13,0} - 13_{12,1}$  and the  $13_{13,1} - 13_{12,2}$  water lines (rest wavelength  $38.0775 \mu\text{m}$  for both lines), has an equivalent width of about  $10 \text{ km s}^{-1}$ . We estimate that absolute errors in the flux calibration of up to  $\pm 20\%$  could result from spacecraft pointing errors (this absolute error being the same in all three FP spectra), and that additional errors of up to  $\pm 30\%$  may result from our fitting of the line profiles. The possible errors in the wavelength calibration correspond to Doppler shifts of up to  $\pm 3 \text{ km s}^{-1}$  for the FP spectra and up to  $\pm 80 \text{ km s}^{-1}$  for the grating spectrum. In GR mode, the water lines are unresolved. In FP mode, the water lines may be partially-resolved, but the instrumental response function is not yet characterized well enough to permit the intrinsic line widths to be determined reliably.

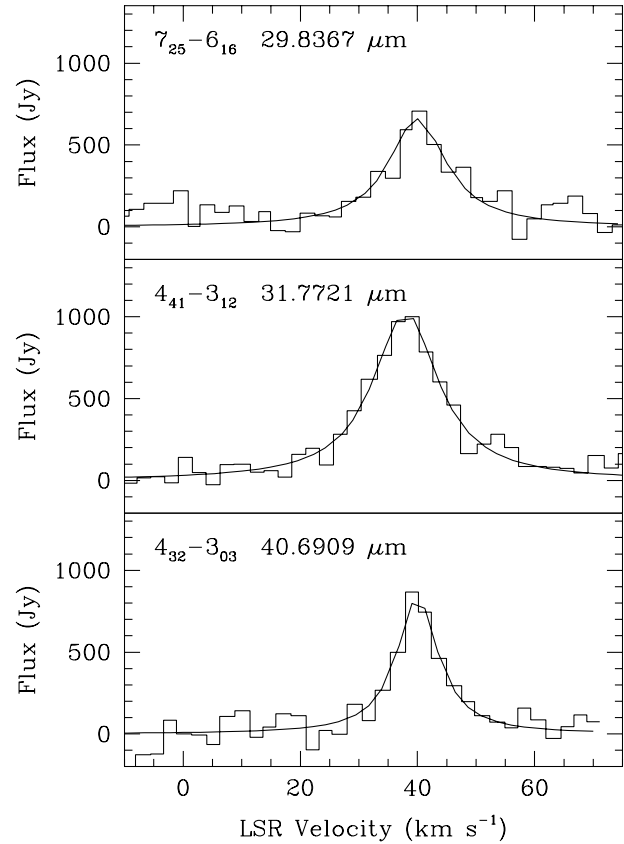


**Fig. 1.** Continuum-subtracted Fabry-Perot spectra of the  $7_{25} - 6_{16}$  line at  $29.8367 \mu\text{m}$ , the  $4_{41} - 3_{12}$  line at  $31.7721 \mu\text{m}$ , and the  $4_{32} - 3_{03}$  line at  $40.6909 \mu\text{m}$ .

### 4. Discussion

We have compared the observed fluxes listed in Table 1 with the predictions of a theoretical model for water emission from circumstellar outflows. Our present treatment extends that described by CN95 by including the radiative pumping of rotational transitions by continuum radiation from dust within the outflow. A model for the dust continuum radiation in W Hyra was kindly provided by S. Doty. We have also improved our treatment of the grain dynamics, assuming the grains to have the size distribution given by Mathis, Rumpl & Nordsieck (1977, hereafter MRN) for *interstellar* grains and the optical properties given by Laor & Draine (1993) for astronomical silicate.

The most important parameters upon which the model predictions depend are the terminal outflow velocity of the gas,  $v_{g\infty}$ , and the gas mass-loss rate,  $\dot{M}_g$ . Line profile observations (Wannier & Sahai 1986, hereafter WS86) provide a fairly reliable determination of the outflow velocity,  $v_{g\infty} = 9.7 \text{ km s}^{-1}$ , but previous studies have not yielded a trustworthy estimate of the gas mass-loss rate. Accordingly, we have treated  $\dot{M}_g$  as a free parameter, and investigated the range of gas mass-loss rates for which acceptable agreement can be obtained for each of the four water lines that we observed. The results of this investigation

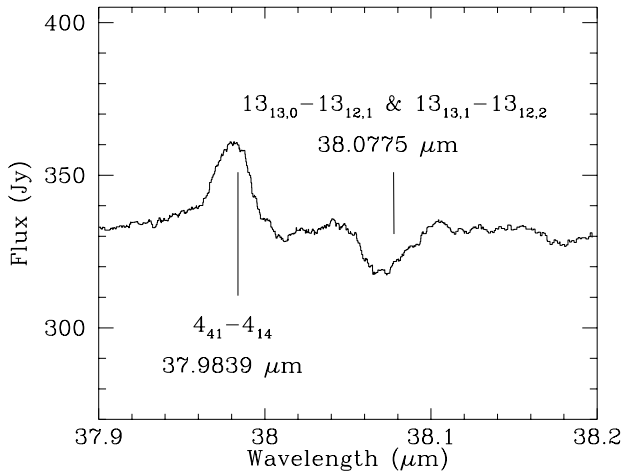


**Fig. 2.** Grating spectrum showing the  $4_{41} - 4_{14}$  emission line at  $37.9839\mu\text{m}$  and a water absorption feature at  $38.0775\mu\text{m}$ . The wavelength scale is in the rest frame of W Hya.

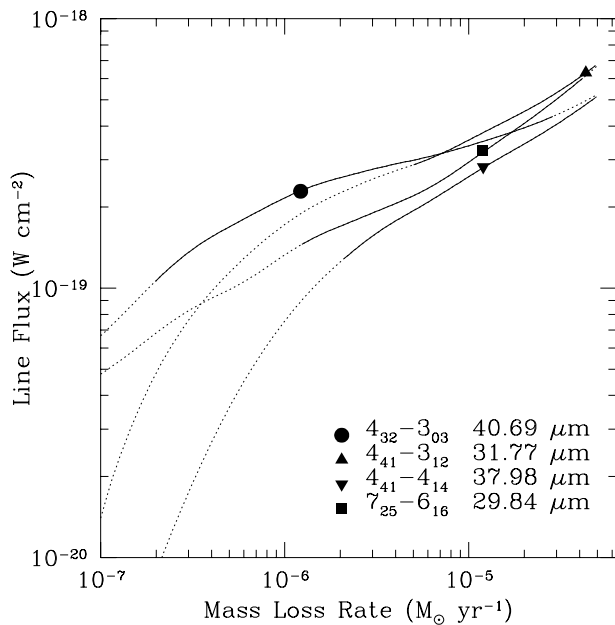


**Fig. 3.** Predicted line fluxes as a function of assumed mass loss rate.

are presented graphically in Figure 3, in which we plot the predicted line fluxes as a function of  $\dot{M}_g$ , for an assumed distance to the source of 95 pc (Haniff, Scholz & Tuthill 1995). Filled symbols on each of the four curves indicate our best estimates of the observed flux, and the solid portions of each curve indicate the range of mass-loss rates for which the predicted flux is in acceptable agreement with the observations, given estimates of  $\pm 20\%$ ,  $\pm 30\%$  and  $\pm 10\%$  respectively for the possible errors in the absolute flux calibration, the line profile fitting, and in the value we adopted for the distance to the source.

Figure 3 indicates that acceptable agreement can be obtained simultaneously for all four emission lines given an assumed gas

mass-loss rate in the range<sup>1</sup>  $\dot{M}_g = (0.5 - 3) \times 10^{-5} M_\odot \text{yr}^{-1}$ . In our model, the peak contribution to the luminosity of the rotational emission lines that we observed occurs at a distance  $\sim 2 - 5 \times 10^{14}$  cm from the star, a region where the gas has an outflow velocity close to its terminal velocity and a kinetic temperature  $\sim 125 - 250$  K.

The gas mass-loss rate that we derived for W Hya by modeling the water line emission is considerably larger than previous estimates in the literature. Estimates in the range  $\dot{M}_g = (0.5 - 2) \times 10^{-7} M_\odot \text{yr}^{-1}$  have been derived (WS86, Loup et al. 1993, Young 1995) from CO observations using the excitation model of Knapp & Morris (1985, hereafter KM85). An independent estimate of the gas mass-loss rate may be obtained from dynamical considerations by determining how large an opacity the outflowing material must have in order to explain the observed gas outflow velocity (e.g. Justtanont, Tielens & Skinner 1994). Applying this method to W Hya, we obtain an estimate  $\sim 1 \times 10^{-3}$  for the dust-to-gas mass ratio; in conjunction with estimates of the dust mass-loss rate derived from observations of far-infrared and submillimeter dust continuum emission (Hawkins 1990; van der Veen et al. 1995), this result implies a gas mass-loss rate in the range  $1 - 3 \times 10^{-6} M_\odot \text{yr}^{-1}$ .

The discrepancies in the estimates of  $\dot{M}_g$  described above may reflect differences in the assumed temperature profiles for the outflowing gas, the CN95 model yielding considerably lower gas temperatures than those derived previously by GS76 and those used as the basis for the KM85 CO excitation model.<sup>2</sup> The fact that the dynamical estimate of  $\dot{M}_g$  lies between the estimates derived using the KM85 and CN95 models may suggest that the true temperature profile of the outflowing gas is intermediate between the temperature profiles computed by GS76 and CN95, a possibility that will be investigated in a future study. Variability in the mass-loss rate is a second possible cause of discrepancies between the various estimates of  $\dot{M}_g$ ; because the water emission region is small compared to the CO emission re-

<sup>1</sup> The uncertainty in the value of  $\dot{M}_g$  quoted here refers only to uncertainties that result from errors in the flux calibration and in the adopted distance to the source. The range of acceptable values would be broadened if we allowed ourselves the liberty to vary other model parameters, such as the assumed rate coefficients for the collisional excitation of  $\text{H}_2\text{O}$  or the assumed properties of the dust in the outflow. In particular, because larger grains show a greater drift velocity relative to the gas and therefore heat the outflow more effectively, the derived mass-loss rate would decrease/increase if the maximum grain radius were assumed to be larger/smaller than the value of  $0.25\mu\text{m}$  that we adopted here (following MRN).

<sup>2</sup> To investigate the dependence of the derived mass-loss rate upon the assumed temperature profile, we redetermined the mass loss rates needed to account for the observed water line strengths using the GS76 temperature profile in place of the temperature profiles that we computed self-consistently for each mass loss rate using the CN95 model. For this case we found that *no* mass-loss rate was able satisfactorily to fit all four transitions, the predicted strength of the  $4_{41} - 4_{14}$  line lying a factor of 6 below its observed value for the mass-loss rate ( $\sim 3 \times 10^{-7} M_\odot \text{yr}^{-1}$ ) that was needed to match the observed fluxes of the other three lines.

**Table 2.** Predicted fluxes in lines for which future ISO observations of W Hydrae are planned

Transition	Wavelength ( $\mu\text{m}$ )	Predicted Line Flux ( $10^{-19} \text{ W cm}^{-2}$ )
$2_{20} - 1_{11}$	100.983	1.5 – 2.1
$4_{14} - 3_{03}$	113.537	1.2 – 1.6
$5_{05} - 4_{14}$	99.493	1.0 – 1.4
$5_{15} - 4_{04}$	95.627	0.8 – 1.3
$6_{42} - 5_{15}$	23.1935	1.2 – 5.4
$5_{50} - 4_{23}$	22.6391	1.6 – 6.1

- Knapp, G. R., & Morris, M. 1985, ApJ, 292, 640 (KM85)  
 Kwok, S. 1975, ApJ, 198, 583  
 Laor, A. & Draine, B. T. 1993, ApJ, 402, 441  
 Loup, C., Forveille, T., Omont, A., & Paul, J.F. 1993, A&AS, 99, 291  
 Mathis, J. S., Rumpl, W., & Nordsieck, K. H. 1977, ApJ, 217, 425 (MRN)  
 Salpeter, E. E. 1974, ApJ, 193, 585  
 Toth, R. A. 1991, J Opt Soc Am B, 8, 2236  
 van der Veen, W. E. C. J., Omont, A., Habing, H. J., & Matthews, H. E. 1995, A&A, 295, 445  
 Wannier, P. G. & Sahai, R. 1986, ApJ, 311, 335 (WS86)  
 Young, K. 1995, ApJ, 455, 872

gion, the water line strengths probe the mass outflow rate for material that has been ejected from the star more recently.

We attribute the absorption feature at  $38.08\mu\text{m}$  to a blend of the  $13_{13,0} - 13_{12,1}$  and  $13_{13,1} - 13_{12,2}$  water lines. These transitions are not included in our model, but the high-lying  $13_{12,1}$  and  $13_{12,2}$  states (with  $E/k = 5882 \text{ K}$ ) presumably attain significant populations only in a small hot region close to the star and are therefore observed in *absorption* against the stellar continuum radiation that dominates the continuum flux at  $38 \mu\text{m}$ .

In summary, our current model for the far-IR water line emission from circumstellar envelopes can account simultaneously for all of the emission line fluxes that we measured, given a gas mass-loss rate in the range  $(0.5 - 3) \times 10^{-5} M_{\odot} \text{ yr}^{-1}$ . In Table 2, we list our model's predictions for the fluxes in other water lines that have not yet been observed but for which future ISO observations are planned. The total flux in all far-IR water emission lines is predicted to be  $\sim 10^{-16} \text{ W cm}^{-2}$ , corresponding to a total luminosity of  $\sim 0.3 L_{\odot}$ . Water emission lines are expected to account for  $\sim 0.4, 1.5$  and  $3\%$ , respectively, of the total 25, 60 and  $100 \mu\text{m}$  IRAS band fluxes.

*Acknowledgements.* We thank S. Doty for his kind assistance in providing us with a model for the dust continuum radiation in W Hya, and G. Knapp for helpful discussions. D.A.N. gratefully acknowledges the hospitality of the University of Maryland, College Park, where he was a sabbatical visitor during the period when this study was carried out. The work of D.A.N. and W.C. was supported by NASA grants NAGW-3147 and NAGW-3183, and that of M.H. was supported by NASA grant NAGW-1261.

## References

- Anders, E., & Grevesse, N. 1989, Geochim. Cosmochim. Acta, 53, 197  
 Bowers, P.F., & Hagen, W. 1984, ApJ, 285, 637  
 de Graauw, T., et al. 1996, A&A, this issue  
 Deguchi, S., & Q-Rieu, N. 1990, ApJ, 360, L27  
 Chen, W., & Neufeld, D.A. 1995, ApJ, 452, L99 (CN95)  
 Gilman, R. C. 1972, ApJ, 178, 423  
 Goldreich, P., & Scoville, N. 1976, ApJ, 205, 144 (GS76)  
 Haniff, C. A., Scholz, M., & Tuthill, P. G. 1995, MNRAS, 276, 640  
 Hawkins, G. W. 1990, A & A 229, L5  
 Justtanont, K., Skinner, C. J., & Tielens, A. G. G. M. 1994, ApJ, 435, 852  
 Kessler, M., et al. 1996, A&A, this issue